ResearchGate

See discussions, stats, and author profiles for this publication at: https://www.researchgate.net/publication/224252878

Design of a low-cost series elastic actuator for multi-robot manipulation

Conference Paper *in* Proceedings - IEEE International Conference on Robotics and Automation · June 2011

DOI: 10.1109/ICRA.2011.5980534 · Source: IEEE Xplore

CITATIONS
6

READS
142

6 authors, including:

Marcia Kilchenman O'Malley
Rice University

200 PUBLICATIONS **2,013** CITATIONS

SEE PROFILE

James Mclurkin
Rice University

41 PUBLICATIONS **864** CITATIONS

SEE PROFILE

Some of the authors of this publication are also working on these related projects:

Project MRI-compatible haptics View project

Project Haptic Paddle View project

All content following this page was uploaded by Marcia Kilchenman O'Malley on 14 March 2014.

The user has requested enhancement of the downloaded file.

2011 IEEE International Conference on Robotics and Automation
Shanghai International Conference Center
May 9-13, 2011, Shanghai, China

Design of a Low-Cost Series Elastic Actuator for Multi-Robot Manipulation

Emma Campbell, Zhao Chad Kong, William Hered, Andrew J. Lynch, Marcia K. O'Malley, James McLurkin

Abstract— **We describe a proof-of-concept design for a low-cost two-degree-of-freedom robotic arm that incorporates series elastic actuators (SEAs) with force sensing. The cost effectiveness of the design will enable the construction of compliant manipulators for multi-robot systems with large populations. The arm assembly attaches to a commercially available mobile robot chassis to perform multi-robot coordination. In this work, we present the design of a robot arm and data from experiments to characterize the accuracy and resolution of the force sensing. We describe a force-following manipulation experiment using two robots. The experiment measures strain on a rigid bar between two robots. The data shows the feasibility of using SEAs for force sensing to reduce the strain in the bar. This is the first step towards a distributed force controller for multi-robot object coordination with large numbers of robots.**

I. INTRODUCTION

In order to realize the potential of multi-robot systems, they must become active participants in the world around them by physically interacting with other objects and manipulating their environment. Multi-robot systems have the ability to manipulate large numbers of objects simultaneously and big objects when working together, but these systems present unique challenges for system design and coordinated control. Our work seeks to address both the hardware and software required to scale multi-robot manipulation to large groups of robots.

There are many robot manipulation tasks that are well-suited for multi-robot systems. For example, a logistics hub (sorting hub, warehouse) might have items of many sizes and shapes. Current systems [1] can manipulate objects on pallets but cannot cooperatively manipulate large objects. A system of cooperative mobile manipulators could dispatch single robots for small items, a few robots for medium items, and a large group of robots for big items. Arguably, the pinnacle of multi-robot manipulation is automated construction [2], which will have an even larger diversity of object sizes, and require six-DOF positioning in unstructured, dynamic environments.

The motivation behind the design of this arm assembly and the development of the governing control laws is inspired by manipulation solutions commonly seen in nature [3], as shown in Figure 1(a). Specifically, we are interested in cooperatively manipulating relatively large objects without the need for explicit communication or position measurements.

Mechanical Engineering Department, Rice University, Houston, TX ecc1,zk1,wah1,omalleym@rice.edu
Computer Science Department, Rice University, Houston, TX lyncas,jmclurkin@rice.edu

(a) Ants cooperatively moving a large object.

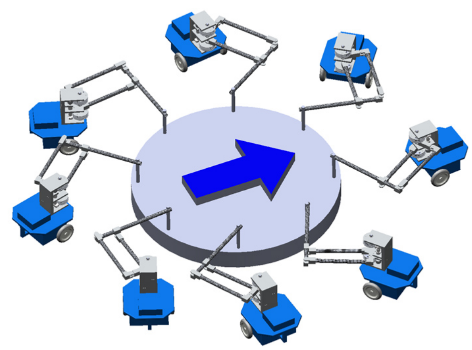

(b) Proposed multi-robot manipulator.

Fig. 1. **a:** Natural systems are able to use large groups of agents for manipulation tasks. The key enabling technologies for this application are force sensing, distributed controllers, and compliant manipulators. **b:** We propose to develop these key concepts to build a multi-robot manipulator.

Instead, we propose to accomplish this task by relying on feedback from sensing forces through the object. We focus on manipulation tasks that require physical interaction with objects of unknown size and configuration. We use compliant actuators to allow the robot to safely interact with its world and to provide force sensing. As shown in Figure 1(b), the goal of our arm design is to provide a test platform suitable for replicating swarm manipulation behavior on multi-robot systems. Our initial robotic system needs accurate force sensing capabilities and low-cost design. Cost is a critical factor for multi-robot manipulation, as any arm design must be replicated in quantity.

Previous manipulation research in multi-robot manipulation has focused on unilateral forces to interact with objects. Pushing of objects has been studied with multi-robot furniture movement tasks [4] and expanded to object closure [5], [6]. Pulling of objects has been studied in two-dimensional systems [7], and three-dimensional aerial manipulation [8]. However, there is little work on bilateral force interactions in large populations, *i.e.* robots that have arms that grasp the object and can both push and pull it. The main challenge to using an arm that is connected to the object is that the positions of all of the robots and their end-effectors cannot be known exactly, so errors in geometry are unavoidable. With rigid manipulators, these geometric errors are intolerable. Additionally, real-world interactions require compliance to protect the robot from the inevitable bumps and collisions involved with cooperative manipulation.

To address these issues, we look towards cooperative manipulation using force control and compliant actuators. We adopt a variant of the leader-follower decentralized cooperative object transportation proposed by Wang [9]. Compliant manipulators allow robot-robot [10] and human-robot interactions [11], [12], with reduced risk of damage to either. This paper focuses on series elastic actuators (SEAs) as the compliant manipulator for multi-robot interaction [13]. Series elastic actuators incorporate an elastic element in the drivetrain of the system, between the gearbox and the end-effector. This elastic element improves the robustness of the system by protecting the gearbox from impact loads and allows the manipulator to make contact with objects in the world without damage to itself or the object. If the elastic element is a linear spring, the force in the joint can be estimated by measuring the displacement between the two ends of the spring. Compliant actuators can also be realized with differential elastic actuators (DEAs) [14], tension based SEAs [15], and rotary series elastic actuators (RSEAs) [16]. Force control of robot manipulators is well studied in the literature [17] and can involve complexities that are outside the scope of this work [18]. This paper focuses on a proof-of-concept series elastic actuator design and a simple transportation task.

The arm design is presented in Section II and experiments to characterize its performance in Section III-A. Since manipulation with large populations of robots is our ultimate goal, we designed a simple multi-robot manipulation experiment to test the force sensing and control abilities of our arm. A force-following experiment is presented in Section III-B.

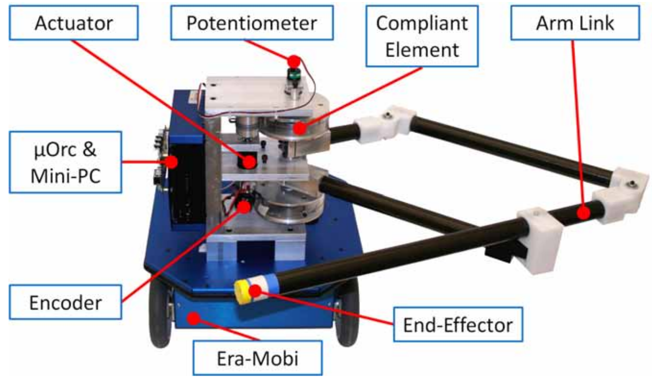

Fig. 2. Our multi-robot manipulator arm mounted on a mobile chassis. Important components and subsystems of the design are highlighted. The arm design uses a five-bar linkage.

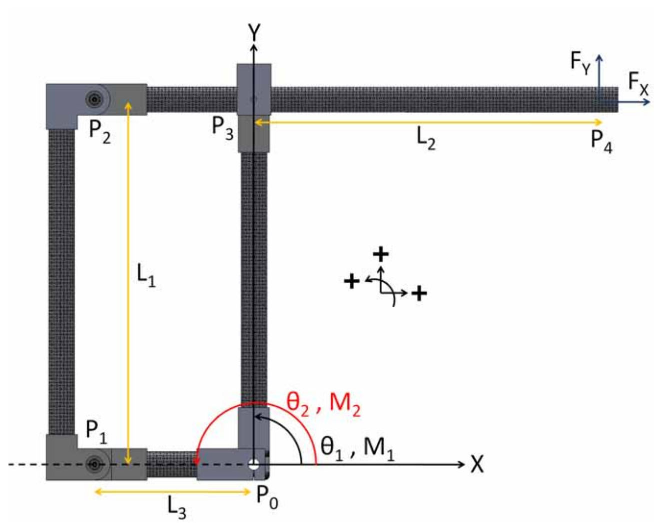

Fig. 3. CAD drawing of the top view of the five-bar linkage. Sign convention and notation used for kinematics. θ_1 & θ_2 correspond to the angles of the two arm links based on potentiometer readings. Arm links are also connected to the SEAs.

II. Arm Design

Our arm design is shown in Figure 2 and is low-cost, easy to build, and uses series elastic actuators. We present the design of the arm assembly in four subsections: arm link design, actuation and sensing, compliant element design, and data acquisition and control.

A. Arm Link Design

The overall design for the arm links is a parallel five-bar linkage [19], [20], shown in Figure 3. This design provides a similar workspace as a shoulder-elbow configuration, but allows for superior mass centralization by placing the heavy drivetrain components for both joints at the shoulder.

Each arm link is made from 1-1/8" carbon fiber tubing with a 1/16" wall thickness. The four arm links are held together with Delrin® joints and pivot on ball bearings. The resulting linkage has high stiffness, low friction, low backlash, and is light weight. The only lateral play in the arm links results from the ball bearings. Each arm link has an effective length of approximately half a meter; when fully extended, this gives the overall arm assembly a one meter radius workspace from the shoulder. This distance provides sufficient clearance between the robot and the object being manipulated.

B. Actuation and Sensing

The motor-gearbox-encoder combination is a trade-off between torque, speed, and cost. We use a 531:1 gearbox (Maxon Planetary Gearhead GP 32, 4.5 Nm), in combination with a 3:1 reduction capstan drive, see Figure 4(a). An integrated 500 count/turn optical quadrature encoder (Maxon HEDS 5540) is attached to each motor (Maxon A-Max 26, 4.5 watt), and measures the relative angular position of the actuator side of the compliant element. Potentiometers (Midori CP-2FK, 5 kOhm) are mounted after the compliant elements, and measure the absolute angular position of the arm links, see Figure 4(b). Once the system is calibrated, we compute an angular displacement across the compliant element, $\theta_{strain} = \theta_{encoder} - \theta_{potentiometer}$. The torque on each joint can be estimated with the transfer function of the compliant element, $\tau = f(\theta_{strain})$. The design has a large linear range, which we demonstrate in Section III-A. This simplifies the above relationship to $\tau = k\theta_{strain}$. The arm links are designed to rotate less than 270 degrees due to the physical limitations of the arm assembly, and the compliant element is designed to deflect no more than 10 degrees under normal operation in order to remain within the linear range of the spring. The entire drivetrain is relatively low cost - the potentiometers are \$33 each, the motor-gearbox-encoder combination are \$360 each, and the rest of the components are \$400, bringing the total parts cost to \$1186. The potentiometers represent the only significant material cost that differentiates the system from a conventional shoulder-elbow manipulator without force sensing. Thus, the system demonstrates that force sensing through the use of SEAs can be incorporated into a system with relatively little cost.

C. Compliant Element Design

Complexity, cost, compactness, and ease of manufacturing were essential criteria in formulating the design for the compliant element. Figure 4(c) shows an exploded diagram of the element, and Figure 4(a) shows the force pathway through the element. From the output shaft of the actuator, the torque is transferred to the outer drum of the compliant element via a capstan drive. The torque is then transferred from the outer drum to the inner shaft of the compliant element via a thin strip of spring steel. Finally, the torque is transferred from the inner shaft to the arm link.

The drum-shaped housing, again in Figure 4(a), contains a strip of spring steel which serves as the compliant element in the SEA. One side of the spring steel is driven by the outer ring of the drum, which is coupled to the output shaft of the gearbox via a capstan drive. The other side of the spring steel is clamped to the inner shaft of the drum and then to the arm link. The thin strip of spring steel is rigidly clamped to the inner shaft and constrained by two ball bearings attached to the outer drum. This removes axial forces from the spring, while allowing bending loads.

The capstan drive between the actuators and the drums minimizes backlash and produces a compact design. The cantilever mounting of the spring steel has several advantages. The clamped-pinned boundary condition for the spring allows deformation to occur while keeping the torque-angle relationship linear. This boundary condition is also symmetric whether rotation occurs clockwise or counter-clockwise. Further, the stiffness of the system can be easily adjusted by changing the thickness of the spring steel. Finally, the components have simple geometries that are easily machined from raw materials.

D. Data Acquisition and Control

Our manipulator is mounted on a Era-Mobi mobile robot chassis by Videre Design and runs the Player/Stage [21] software system. For the following experiments, we designed a Java client to communicate with the Player server and control the robot. The entire robot and arm are fully autonomous and untethered; they run off the Era-Mobi's onboard battery supply.

The μOrc board [22] is used for sensing and motor control of the arm assembly. The μOrc board is based on the 50 MHz, 32-bit, LM3S8962 microcontroller from Texas Instruments. The μOrc board comes with motor controllers, quadrature encoder inputs, and analog input channels. The driver software interfaces easily to a Java API for rapid prototyping of control software.

III. Experimentation and Results

We perform two experiments to demonstrate the feasibility of the design for performing more complex multi-robot manipulation tasks. The first experiment characterizes the accuracy and linearity of our system in a controlled environment. The second experiment demonstrates manipulation of an object by two robots.

A. Characterization

To characterize the accuracy and linearity of the force sensing, we placed the arm assembly in a fixed position. Known masses, ranging from 0.5 kg to 2.0 kg in 0.5 kg increments, were used to apply a force to the arm. A pulley was used to apply this force in the plane parallel to the ground.

Before operation, the arm must be initialized to correlate the encoder positions and the potentiometer positions. The potentiometers can measure absolute angular position of each arm link, but the encoders can only measure relative position. Thus a reference encoder reading must be correlated to an initial potentiometer reading. This initialization step must be done with no force on the compliant element. Because of this need to correlate, mechanical play in the system introduces errors in the force sensing capabilities. Mechanical play in the planetary gearboxes used in the two actuators is the main source of this error. In order to identify the effect of this mechanical play on the accuracy of the system, initialization of the system was done deliberately. In the first characterization test, the arm was reinitialized before each weight was applied, and 12 data points were taken at each force increment for a total of 48 data points. There are a total of four backlash states in the system; two for each actuator. Prior to each initialization, the system was returned to its pose in a specific way as to reach each of the four backlash states. This provides careful measurement of the force sensing accuracy of the system since reinitialization occurs after each load is applied and the system is deliberately put into each of the four backlash states.

However, this is not representative of normal operation. Under normal autonomous operation, initialization would occur infrequently and in an unknown backlash state. In

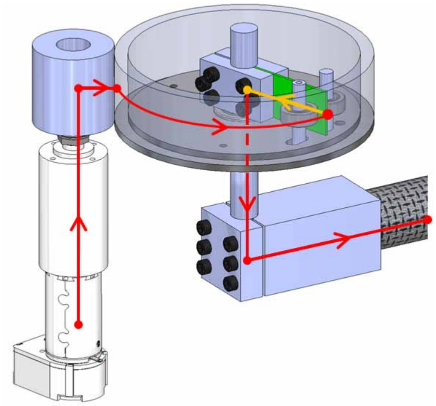

(a) Force pathway from encoder to arm link. Capstan wire between actuator and compliant element not pictured.

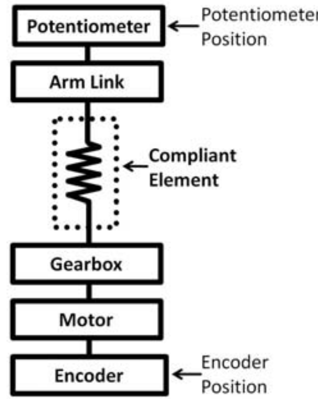

(b) Block diagram of SEA.

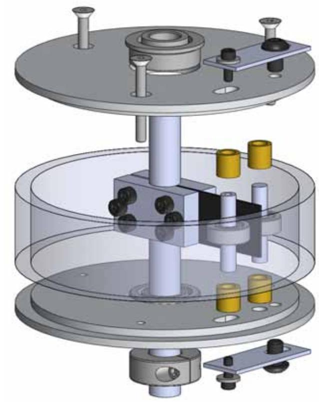

(c) Exploded view of compliant element.

Fig. 4. **a:** Torque propagation diagram of the SEA. The red arrows show transfer of force through rigid elements. The yellow arrow shows transfer of force through the compliant element. The spring steel is shown in green; the capstan wire is not pictured. **b:** System schematic for one SEA. The spring between the motor and the arm link adds compliance to the system. Using the differential between the potentiometer and encoder positions allows us to estimate the torque on the joint. **c:** Exploded view of the rotary compliant element in the SEA. The thin strip of spring steel, shown in black, is rigidly clamped to the center shaft. The spring is 'pinned' to the outer drum by a set of roller bearings, creating a cantilever.

the second characterization test, the arm was initialized only once for each sequence of weights for a total of six trials. This provides a better view of the linearity and accuracy of the design when it is running autonomously.

The data collected from the first test are shown in Figure 5. The curve for an ideal spring is shown in black. For a particular force applied, the variability in the force measured data represents errors caused by the mechanical play in the system. The planetary gearbox used in the actuators is the main source of mechanical play. The potentiometers are able to measure the mechanical play because they are positioned after the gearbox, but the encoders are unable to correct for this, see Figure 4(b). This mechanical play adds error to the force measurements. These inaccuracies manifest themselves when the system is initialized because the reference encoder reading for the zero-force state is taken during initialization. The use of a low-backlash geartrain, such as a harmonic drive, would reduce this error but would greatly increase the cost of the system. Thus, this error is a necessary concession for the use of the lower-cost planetary gearboxes.

The data from the second test, Figure 6, demonstrate the performance under more realistic operating conditions. The system is reinitialized only once for each trial. The data fit a linear regression with an average R-squared value of 0.99945. However, the lines are offset from the origin. The range of these offsets correspond to the measurements of mechanical play from the first experiment. We conclude that the spring design is linear and that mechanical play is the largest source of force measurement error.

B. Mobile Manipulation Experiment

Our ultimate goal is multi-robot distributed manipulation using force sensing. To demonstrate the feasibility of this new design in this application, we conducted a simple experiment with a pair of robots manipulating a flexible

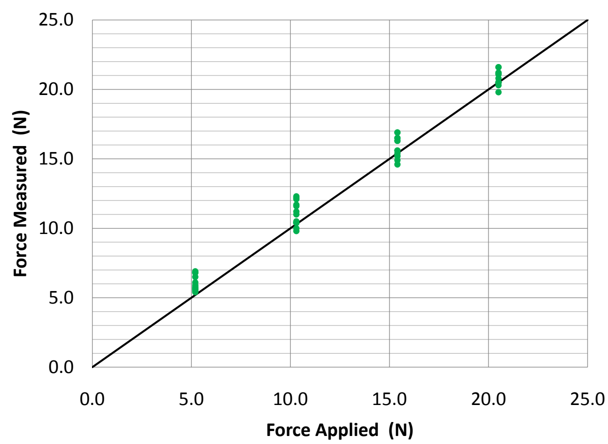

Fig. 5. Force measured versus force applied for the first set of characterization tests when the system was reinitialized before each weight was applied.

aluminum bar. The *actuated robot* consists of the previously described arm assembly attached to an Era-Mobi chassis. The *unactuated robot* consists of the same model chassis with a rigid mounting bracket for the bar. Two different tests were conducted. In the control test, the arm assembly was not used at all. Both robots had rigid brackets that allowed the bar to be clamped between each robot. The bar was clamped so that it would be perpendicular to the intended path of travel as shown in Figure 8(a). Both robots were driven in a straight line with the same sinusoidal velocity profile, and were kept in sync via a wireless. The amount of deflection in the aluminum bar connecting the robots was recorded by a stain gauge. Prior to experimentation, the strain gauge was calibrated using a three-point bending setup. Voltage from

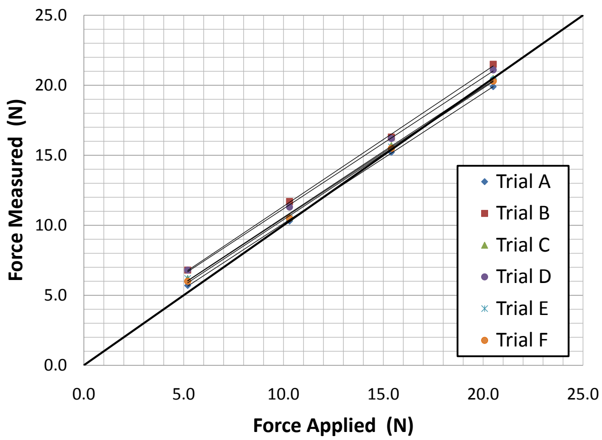

Fig. 6. Force measured versus force applied for the second set of characterization tests when the system was initialized only at the beginning of each trial.

the strain gauge was mapped to deflection at the mid-point of the bar. The calibration relationship was linear with a R-squared value of 0.997. This relationship was then used to plot the deflection in the bar versus time.

In the second test, the aluminum bar was clamped to the unactuated robot via a bracket while the other end of the bar was clamped directly to the arm assembly on the actuated robot, see Figure 7. The attachment point on the arm was rigidly clamped, *i.e.* the bar could not rotate, and all forces and torques were transmitted to the arm. The unactuated robot was sent velocity commands, identical to those in the control test. The actuated robot was put in a mobile manipulation mode. In this mode, the actuated robot kept the arm assembly in a fixed pose. The forces measured at the end-effector were used as the input signal for a simple proportional controller. Output from this proportional controller was then used as velocity signals for the chassis of the actuated robot. The actuated robot followed the forces sensed at its end-effector as the unactuated robot followed the same fixed path as in the control test. The amount of deflection in the bar was recorded.

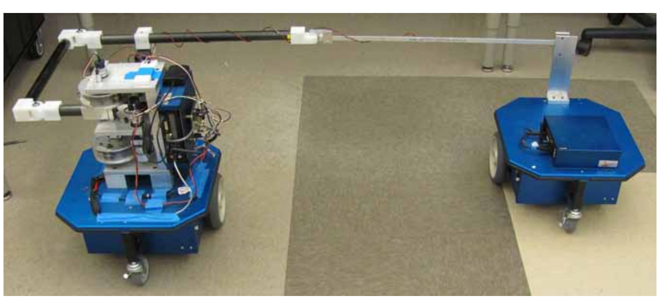

Fig. 7. Force-following experiment with compliant robotic arm attached by flexible aluminum bar to unactuated mobile robot.

The deflection sensor measurements are plotted in Figure 9 against time for five actuated and five unactuated trials.

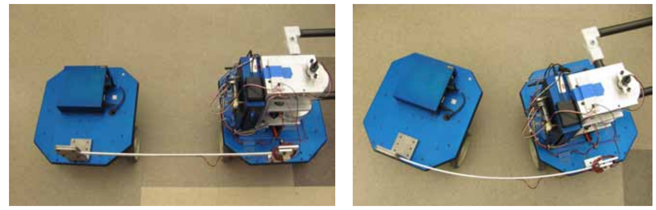

(a) Undeflected (b) Deflected

Fig. 8. **a:** Nominal case when bar is undeflected, representative of 0 cm of deflection. **b:** Deflected case during straight line travel of two unactuated robots, representative of 3 cm of deflection.

Figures 8(a) and 8(b) show representative pictures of 0 cm and 3 cm of deflection respectively. Figure 10 shows the position of the actuated robot and unactuated robot based on encoder readings from the driven wheels. Slippage between the ground and the driven wheels causes a discrepancy between the encoder readings and the actual displacements observed. In the control trial, both robots received identical velocity signals. Their paths deviated towards each other due to imperfect initial alignment, resulting in large deflections in the bar, as in Figure 8(b). In the actuated experiment where the actuated robot was not sent an explicit velocity signal but used the arm assembly to sense forces from the bar, much lower levels of deflection were observed in the bar as shown in Figure 9. Oscillations can be observed both in the signals from the deflection sensor and the encoder positions because a simple proportional controller was used.

In summary, the arm's torque sensor is linear and the actuated robot was able to use the force sensing capabilities of the arm assembly to follow the position of the unactuated robot. Additionally the results demonstrate that the actuated robot is able to use the force sensing capabilities of the arm assembly to perform the task more successfully; the amount of deflection observed in the bar is decreased by approximately 75%.

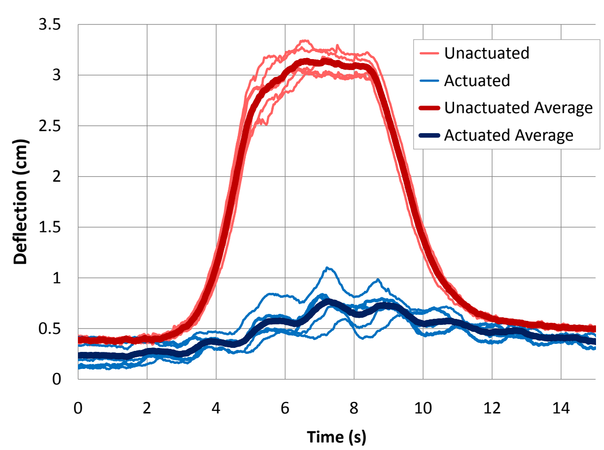

Fig. 9. Beam deflection versus time for both actuated and unactuated test cases, see Figure 8 for deflection scale. Average values for these trails are included.

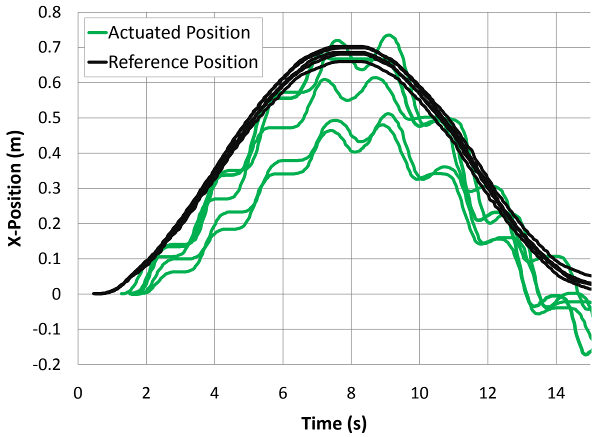

Fig. 10. Position of robots as a function of time. Black curves show the position for the robots when they are both sent the same velocity signals. Green curves show the position of the actuated robot when in mobile manipulation mode. Measurements were made by wheel encoder readings on the Era-Mobi. Due to oscillatory motion of the robot under mobile manipulation mode, more wheel slippage was experienced than in the control case.

IV. Conclusions and Future Work

This paper presents the design of a low-cost series elastic actuator for mobile multi-robot manipulation. The force is estimated from the difference of two position measurements and a calibrated spring. Basic characterization tests show the design is linear and performs well. A simple multi-robot manipulation experiment shows a large reduction in deflection of the manipulated object, and the ability of the arm to control position using force sensing.

Our compliant robotic arm assembly is the first step towards a research system for cooperative multi-robot manipulation. Our next steps are to properly characterize the system and design a force controller and impedance controller [23]. We focused on low-cost gearboxes for this iteration, but are interested in investigating a low-cost, low-backlash drive-train. This prototype design can also be simplified to make it more compact and easier to assemble. We will need to produce many more prototypes in order to perform a large-scale manipulation experiment. However, the most important next step is the design of a distributed controller to allow the entire population of robots to reach consensus on their force vectors using force-feedback [24]. This will allow us to achieve efficient manipulation of a large object in a distributed fashion.

References

[1] P. W. Raffaello D'Andrea, "Future challenges of coordinating hundreds of autonomous vehicles in distribution facilities," in *IEEE Technologies for Practical Robot Applications, TePRA 2008*, (Woburn, MA), Nov. 2008.

[2] K. Galloway, R. Jois, and M. Yim, "Factory floor: A robotically reconfigurable construction platform," in *Robotics and Automation. Proceedings. 2010 IEEE International Conference on*, pp. 2467–2472, May 2010.

[3] S. Berman, Q. Lindseyy, M. S. Sakary, V. Kumary, and S. Prattz, "Study of group food retrieval by ants as a model for multi-robot collective transport strategies," *Robotics Science and Systems*, 2010.

[4] D. Rus, B. Donald, and J. Jennings, "Moving furniture with teams of autonomous robots," in *Proceedings of IEEE/RSJ International Conference on Intelligent Robots and Systems*, pp. 235–242, 1995.

[5] J. Esposito, "Decentralized cooperative manipulation with a swarm of mobile robots," in *Proceedings 2009 IEEE/RSJ International Conference on Intelligent Robots and Systems*, (St. Louis, MO), pp. 5333–5338, 2009.

[6] Z. Wang and V. Kumar, "Object closure and manipulation by multiple cooperating mobile robots," in *Proceedings of IEEE International Conference on Robotics and Automation*, pp. 394–399, 2002.

[7] P. Cheng, J. Fink, and V. Kumar, "Cooperative towing with multiple robots," *ASME Transactions: Journal of Mechanisms and Robotics*, vol. 1, Feb. 2009.

[8] N. Michael, J. Fink, and V. Kumar, "Cooperative manipulation and transportation with aerial robots," in *Robotics Science and Systems*, (Seattle, WA), Jun. 2009.

[9] Z.-D. Wang, Y. Takano, Y. Hirata, and K. Kosuge, "A pushing leader based decentralized control method for cooperative object transportation," in *Intelligent Robots and Systems. (IROS 2004). Proceedings. 2004 IEEE/RSJ International Conference on*, vol. 1, pp. 1035–1040, Sept. 2004.

[10] L. Chaimowicz, T. Sugar, V. Kumar, and M. Campos, "An architecture for tightly coupled multi-robot cooperation," in *Robotics and Automation. Proceedings 2001 ICRA. IEEE International Conference on*, vol. 3, pp. 2992–2997, 2001.

[11] M. Zinn, O. Khatib, B. Roth, and J. K. Salisbury, "Playing it safe: A new actuation concept for human-friendly robot design," *IEEE Robotics and Automation Magazine*, vol. 11, no. 2, pp. 12–21, 2004.

[12] C. Kemp, A. Edsinger, and E. Torres-Jara, "Challenges for robot manipulation in human environments," *Robotics Automation Magazine, IEEE*, vol. 14, pp. 20–29, Mar. 2007.

[13] G. A. Pratt and M. Williamson, "Series elastic actuators," in *Proceedings of IEEE/RSJ International Conference on Intelligent Robots and Systems*, vol. 1, (Pittsburg, PA), pp. 399–406, 1995.

[14] M. Lauria, M. Legault, M. Lavoie, and F. Michaud, "Differential elastic actuator for robotic interaction tasks," *IEEE International Conference on Robotics and Automation. Proceedings*, pp. 3606–3611, 2008.

[15] J. Sulzer, M. Peshkin, and J. Patton, "Marioonet: An exotendon-driven rotary series elastic actuator for exerting joint torque," in *Rehabilitation Robotics. ICORR 2005. 9th International Conference on*, pp. 103–108, Jun. 2005.

[16] K. Kong, J. Bae, and M. Tomizuka, "Control of rotary series elastic actuator for ideal force-mode actuation in human-robot interaction applications," *Mechatronics, IEEE/ASME Transactions on*, vol. 14, pp. 105–118, Feb. 2009.

[17] O. Khatib, "A unified approach for motion and force control of robot manipulators: The operational space formulation," *IEEE Robotics and Automation*, vol. 3, no. 1, pp. 43–53, 1987.

[18] A. Schneider, H. Cruse, and J. Schmitz, "A biologically inspired active compliant joint using local positive velocity feedback (LPVF)," *IEEE Transactions on Systems and Cybernetics*, vol. 35, no. 6, pp. 1120–1130, 2005.

[19] C. Perry, "Design of a high performance robot for use in haptic interface and force feedback," Master's thesis, Vanderbilt University, 1997.

[20] D. Wang and M. Vidyasagar, "Modelling of a 5-bar-linkage manipulator with one flexible link," in *Robotics and Automation. Proceedings. 1988 IEEE International Conference on*, vol. 1, pp. 21–26, Apr. 1988.

[21] A. H. B Gerkey, RT Vaughan, *The Player/Stage Project: Tools for Multi-Robot and Distributed Sensor Systems*, pp. 317–323. ICAR, 2003.

[22] E. Olson, "uorc specifications and reference documents." available at `http://orcboard.org/`, 2010.

[23] G. Pratt, P. Willisson, C. Bolton, and A. Hofman, "Late motor processing in low-impedance robots: Impedance control of series-elastic actuators," in *American Control Conference. 2004 Proceedings*, vol. 4, pp. 3245–3251, Jun. 2004.

[24] R. Olfati-Saber, J. Fax, and R. Murray, "Consensus and cooperation in networked Multi-Agent systems," *Proceedings of the IEEE*, vol. 95, no. 1, pp. 215–233, 2007.

View publication stats